Low-temperature heat capacities of synthetic pyrope, grossular, and pyrope$_{60}$grossular$_{40}$

H. T. Haselton, Jr*

Department of the Geophysical Sciences, University of Chicago, Chicago, IL 60637, U.S.A.

and

E. F. Westrum, Jr

Department of Chemistry, University of Michigan, Ann Arbor, MI 48109, U.S.A.

Abstract—The heat capacities of synthetic pyrope (Mg$_3$Al$_2$Si$_2$O$_{12}$), grossular (Ca$_3$Al$_2$Si$_3$O$_{12}$), and a solid solution pyrope$_{60}$grossular$_{40}$ (Mg$_{1.8}$Ca$_{1.2}$Al$_2$Si$_3$O$_{12}$) have been measured by adiabatic calorimetry in the temperature range 10–350 K. The samples were crystallized from glasses in a conventional piston–cylinder apparatus.
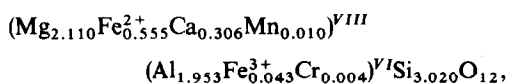
The molar thermophysical properties at 298.15 K (J mol^{-1} K^{-1}) are:

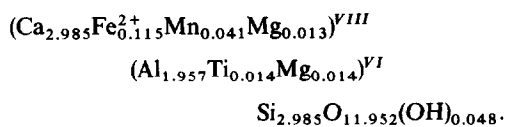|	C_p°	$S_{298}^\circ - S_0^\circ$	$H_{298}^\circ - H_0^\circ/T$
Pyrope	325.31	266.27	47852
Grossular	333.17	260.12	47660
Py$_{60}$Gr$_{40}$	328.03	268.32	47990

The values for the end members are significantly greater than those presented previously for natural samples of pyrope and grossular. The pyrope$_{60}$grossular$_{40}$ exhibits an excess heat capacity below 120 K; the maximum occurs at 45–50 K. The anomalously high heat capacity of pyrope at low temperatures and the excess heat capacity of the solid solution are apparently caused by the unusually large, eight-fold coordination of Mg^{2+} in the garnet structure.

INTRODUCTION

Garnets occur in a wide variety of geological environments and participate in reactions that can serve as pressure and temperature indicators, thus the thermodynamics of garnet solid solutions are of considerable petrologic interest. Thermophysical data for the pure end members are needed to evaluate the mixing relations in natural garnets. Unfortunately, with the exception of data on two natural samples, there are no measurements of low-temperature heat capacities for geologically important compositions. Kolesnik *et al.* (1977) report data for a pyrope-rich garnet

$$(Mg_{2.110}Fe^{2+}_{0.555}Ca_{0.306}Mn_{0.010})^{VIII}$$

$$(Al_{1.953}Fe^{3+}_{0.043}Cr_{0.004})^{VI}Si_{3.020}O_{12},$$

but only the heat capacity at 298 K was adjusted to the end-member composition. Westrum *et al.* (1979) measured heat capacities from 5–600 K on a natural, gem-quality grossular of composition

$$(Ca_{2.985}Fe^{2+}_{0.115}Mn_{0.041}Mg_{0.013})^{VIII}$$

$$(Al_{1.957}Ti_{0.014}Mg_{0.014})^{VI}$$

$$Si_{2.985}O_{11.952}(OH)_{0.048}.$$

---

* U.S. Geological Survey, 959 National Center, Reston, VA 22092, U.S.A.

In both of the above studies, compositional corrections were necessary for impurities whose thermodynamic properties had to be estimated.

Enthalpies of solution (ΔH_{soln}) measured recently for synthetic garnets on the pyrope–grossular join by NEWTON *et al.* (1977a) at 970 K in a 2PbO·B$_2$O$_3$ melt show a positive deviation from ideality for the enthalpy of mixing (ΔH_{mix}), with a maximum of ~9 kJ mol^{-1} displaced slightly toward pyrope-rich compositions. Heat capacities in the range 350–1000 K have been measured by differential scanning calorimetry for synthetic pyrope (NEWTON *et al.*, 1977b), and synthetic and natural grossular (KRUPKA *et al.*, 1979). Relative enthalpy measurements using a Tian–Calvet microcalorimeter have been reported over a similar temperature range for natural samples of pyrope and grossular (TOPOR *et al.*, 1972; KISELEVA *et al.*, 1972).

Garnets of rocks in much of the lower crust and upper mantle are rich in pyrope and grossular components, thus the thermophysical properties of these end members are of particular importance. The apparent anomalously high entropy of pyrope (NEWTON *et al.*, 1977a) and a postulated excess entropy of mixing for solid solutions on the pyrope–grossular join (HENSEN *et al.*, 1975), inferred from phase equilibrium calculations, are additional reasons for the direct measurement of low-temperature heat capacities.

Table 1. Cell edges of synthetic garnets. Uncertainties are least squares standard errors (1σ)

Sample	a_o(nm)	Peaks	Int. Std.
Pyrope	1.14540(5)	15	silicon
Grossular	1.18507(3)	20	spinel
Pyrope$_{60}$grossular$_{40}$	1.1628(1)	17	spinel

Heat capacities for synthetic pyrope ($Mg_3Al_2Si_3O_{12}$), grossular ($Ca_3Al_2Si_3O_{12}$), and pyrope$_{60}$grossular$_{40}$ ($Mg_{1.8}Ca_{1.2}Al_2Si_3O_{12}$) have been measured to examine the possibility of excess heat capacity in solid solutions as well as to provide low-temperature thermophysical data on the end-members.

SAMPLE PREPARATION

Pyrope

An oxide mix was prepared from MgO (single crystal periclase, Muscle Shoals Electrochemical Corp.), Al(OH)$_3$ (Fisher, reagent grade), and $SiO_2 \cdot nH_2O$ (Baker, reagent grade). All reagents were initially fired at 1675 K for 4–6 hr and cooled in a desiccator containing Drierite immediately prior to weighing. All mixing, here and below, was done with a corundum mortar and pestle. The oxide mix was fused at 1875 K for 10 min in 325–350 mg portions. The melt was quenched to a glass in a Hg bath and was subsequently homogenized by crushing and regrinding, again, with a corundum mortar and pestle. The glass was crystallized in graphite containers (1623–1673 K, 30 kbar, 1 hr, 215 mg per run) in a conventional piston–cylinder apparatus.

Grossular

The oxide mix was prepared from CaCO$_3$ and Al$_2$O$_3$ (Baker, Ultrex grade) and SiO$_2$ (acid-leached, natural quartz, Lisbon, Maryland). The CaCO$_3$ was dried at 383 K for at least 48 hr. The firing of the oxides was the same as for the pyrope sample. The mix was decarbonated at 1023 K and fused at 1673 K for 1 hr. The glass was homogenized by crushing and regrinding and was crystallized (1523 K, 25 kbar, 3 hr, 500–600 mg/batch in graphite containers).

Pyrope$_{60}$grossular$_{40}$

The oxide mix was prepared from CaCO$_3$ and Al$_2$O$_3$ (Baker, Ultrex grade), MgO (single crystal periclase, Muscle Shoals Electrochemical Corp.), and SiO$_2$ (acid-leached, natural quartz, Lisbon, Maryland. The drying procedure and decarbonation were the same as above. The mix was fused at 1773 K for 1.5 hr. Approximately one-third of the crushed and remixed glass was crystallized at 1573 K and 40 kbar for 1 hr in graphite containers. The balance was surrounded by a matrix of graphite and invar and was crystallized at 1623 and 46 kbar in Professor George C. Kennedy's laboratory at the University of California at Los Angeles. After the removal of the matrix. electron microprobe analyses of the garnet at the edges of several chips gave FeO concentrations of less than 0.03%.

Many of the early runs made on the pyrope$_{60}$grossular$_{40}$ were contaminated with aluminous clinopyroxene, apparently stabilized by the small amounts of Na$_2$O in ordinary reagent grade chemicals. This problem was resolved by using high purity reagents and 20% seeding.

Graphite was removed from the samples by oxidation in air at 1023 K. The graphite–invar matrix was removed by alternating treatments with KNO$_3$ + H$_2$SO$_4$ and HNO$_3$ + HCl. No sign of gelatinization could be detected in garnet chips subjected to this treatment.

The crystallized garnet used for the heat capacity determinations was in the form of translucent discs (6–8 mm dia) and chips composed of aggregated crystals 5–10 μm in dimension. Microscopic examination showed very small amounts of an unidentified birefringent material in some of the chips, but when present the concentration was estimated to be much less than 1%. All peaks in the X-ray diffraction scans were attributable to garnet.

The cell parameters, presented in Table 1, were refined from powder diffraction data (BURNHAM, 1962). The data were obtained using Cu K$_\alpha$ radiation at a scan rate of 1/8° 2θ min^{-1}. U.S. National Bureau of Standards (NBS) silicon and spinel [a_o = 0.80839(3) nm, refined with NBS silicon] were used as internal standards. The positive deviation [0.0015(1) nm] of the pyrope$_{60}$grossular$_{40}$ unit cell edge from a linear combination of the end member values is in excellent agreement with that found by NEWTON et al. (1977a).

Chemical analyses of the garnets were obtained with the ARL electron microprobe equipped with a solid state detector at the University of Chicago. It is our experience (also R. C. NEWTON, personal communication, 1979) that good analyses of synthetic, fine-grained aggregates, such as the present materials, are difficult due to the problem of distinguishing grain boundaries with the electron microprobe optics. With this cautionary note, averaged analyses of at least 10 spots for each sample are listed in Table 2.

Table 2. Electron microprobe analyses of synthetic garnets

Composition		CaO	MgO	Al$_2$O$_3$	SiO$_2$	Sum
Pyrope	Probe		30.05	25.49	45.06	100.60
	Theoretical		30.00	25.29	44.71	100.00
Grossular	Probe	36.79		22.40	39.51	98.70
	Theoretical	37.35		22.64	40.01	100.00
Py$_{60}$Gr$_{40}$	Probe	15.85	17.22	24.75	42.69	100.51
	Theoretical	15.94	17.19	24.16	42.71	100.00

The compositional range of the pyrope$_{60}$grossular$_{40}$ was estimated to be ± 1–$2\,\text{mol}\%$ by visual examination of the shape and width of high-angle diffractions. The limited number of electron microprobe analyses are compatible with this conclusion.

The sample masses *in vacuo* were 9.7596, 10.1420, and 9.7926 g for pyrope, grossular, and pyrope$_{60}$grossular$_{40}$, respectively. The formula weights used in the calculations were 403.127, 450.452, and 422.057 g mol^{-1} for pyrope, grossular, and pyrope$_{60}$ grossular$_{40}$, respectively and are based on the 1975 values for the atomic weights (Commission on Atomic Weights. 1976).

CALORIMETRY

The same calorimeter (laboratory designation W-34) with a mass of 10.61 g was used for all heat capacity measurements. After loading and evacuation, a small measured amount of purified helium was added to promote thermal equlibration. The amounts of Apiezon-T grease, helium, and solder used for the measurements of the garnet samples closely match those used during the measurement of the heat capacity of the empty calorimeter, which was redetermined as a part of the present investigation. Corrections for differences in the masses of the above materials were small in comparison with the accuracy of the final results. When the end-member samples were measured, the fraction of the total heat capacity (calorimeter + sample) attributed to the samples increased from approximately 0.03 at 10 K, to 0.3 at 100 K, and to 0.5 at 350 K. The values for the pyrope$_{60}$grossular$_{40}$ sample were similar except at 10 K where the fraction was 0.14.

The heat capacity measurements were made in the Mark II adiabatic cryostat described elsewhere (WESTRUM *et al.*, 1968). A capsule-type platinum resistance thermometer (laboratory designation A-5) was used for temperature determinations. All determinations of mass, current, voltage, time, and temperature were referred to calibrations or standardizations performed by the U.S. National Bureau of Standards.

RESULTS

The experimental heat capacity values for pyrope, grossular, and pyrope$_{60}$grossular$_{40}$ are presented in Tables 3–5 in chronological sequence at the mean temperatures of the determinations. Temperature increments employed in the measurements can be inferred from the differences in the adjacent mean temperatures. The heat capacities have been adjusted for curvature to correct for the finite temperature increment of each measurement. The standard deviations of the heat capacities from polynomials, fitted by least squares, are $<5\%$ below 50 K, $<1\%$ from 50–100 K, and $<0.1\%$ above 100 K except for grossular for which the percentage is 0.15 above 100 K. The data for pyrope$_{60}$grossular$_{40}$ are plotted in Fig. 1. For clarity only the fitted polynomials are shown for the end-member compositions. In addition, the smoothed values of KOLESNIK *et al.* (1977) for a natural pyrope sample are plotted below 50 K for comparison.

At the lowest temperatures the heat capacities were fitted to an equation of the form $C_p = \alpha T^3$ to permit extrapolation of the measured data to zero Kelvin. This extrapolation accounts for less than 0.01% of the entropy function at 298.15 K. The results for each

Table 3. Experimental heat capacities of pyrope, $Mg_3Al_2Si_3O_{12}$

Temp K	Heat Capacity J mol^{-1}K^{-1}	Temp K	Heat Capacity J mol^{-1}K^{-1}
Series 1		Series 4	
63.84	39.188	8.20	0.085
69.38	46.80	9.47	0.072
75.54	55.58	10.72	0.091
82.34	66.31	11.78	0.052
89.69	78.19	12.81	0.103
97.79	90.40	14.00	0.127
106.91	105.20	15.39	0.493
116.62	120.82	17.02	0.497
Series 2		18.89	0.652
115.59	118.99	20.50	0.948
125.44	134.69	22.42	1.334
134.84	149.07	24.50	2.029
144.20	162.91	26.89	2.821
153.70	176.80	29.41	3.939
163.33	190.13	31.82	5.162
173.00	203.14	34.33	6.760
182.61	215.49	37.22	8.871
192.28	226.83	40.36	11.419
202.15	238.29	43.38	14.130
Series 3		46.51	17.284
210.50	247.10	50.32	21.469
220.43	257.93	54.66	26.662
230.41	268.13	59.32	32.543
240.31	277.87	64.47	39.713
250.20	286.79	70.21	47.66
260.12	295.23	Series 5	
		264.57	298.48
		275.03	307.97
		286.39	317.23
		297.15	324.71
		307.39	331.17
		317.19	338.55
		326.65	344.75
		335.74	351.03
		345.06	357.00

Table 4. Experimental heat capacities of grossular, $Ca_3Al_2Si_3O_{12}$

Temp K	Heat Capacity J mol^{-1}K^{-1}	Temp K	Heat Capacity J mol^{-1}K^{-1}
Series 1		Series 3	
129.79	137.06	11.45	0.074
135.05	145.46	13.18	0.105
144.12	159.91	14.92	0.333
153.68	174.33	16.83	0.457
162.33	187.38	18.89	0.607
171.21	200.31	20.92	0.941
180.34	212.63	22.87	1.223
189.19	219.29	25.03	1.743
198.00	235.69	27.47	2.316
206.77	245.32	30.17	3.173
215.87	255.66	33.34	4.556
225.46	266.12	36.50	6.248
Series 2		39.43	7.939
211.48	249.40	42.54	10.209
217.70	253.83	45.70	12.676
228.00	269.30	49.39	16.063
239.30	280.40	53.78	20.166
250.94	295.39	Series 4	
262.35	299.14	56.55	23.905
272.86	311.32	61.06	29.437
282.43	321.73	66.45	36.479
302.55	335.84	71.92	43.57
312.73	344.52	78.09	52.62
322.74	351.46	85.26	64.25
332.62	358.39	92.98	76.41
343.42	365.14	102.09	91.12
		111.75	107.02
		120.62	122.16
		129.78	137.08
		139.40	152.26

Table 5. Experimental heat capacities of pyrope$_{60}$ grossular$_{40}$, Mg$_{1.8}$Ca$_{1.2}$Al$_2$Si$_3$O$_{12}$

Temp K	Heat Capacity J mol^{-1}K^{-1}	Temp K	Heat Capacity J mol^{-1}K^{-1}
Series 1		284.45	318.26
53.97	27.063	294.61	325.09
58.64	32.505	304.64	332.79
63.85	38.979	314.18	339.47
68.99	45.80	323.81	346.26
75.52	54.84	333.99	353.05
83.23	66.77	344.31	360.80
90.88	78.76	Series 4	
99.59	91.87	7.89	0.018
108.75	106.50	9.65	0.247
118.26	121.62	Series 5	
127.33	136.32	5.68	0.027
137.08	151.30	6.50	0.030
147.54	167.03	8.08	0.080
Series 2		9.60	0.193
136.29	149.85	11.11	0.561
146.21	164.98	13.05	0.239
156.40	179.70	14.84	0.732
166.37	194.14	16.69	1.173
176.18	207.16	18.93	1.695
185.89	219.69	21.53	2.586
195.56	231.37	24.44	3.664
205.34	242.70	27.74	5.200
215.06	253.63	30.74	6.840
224.79	263.45	33.45	8.522
234.66	273.35	36.30	10.619
Series 3		39.19	12.756
224.31	262.95	42.34	15.319
234.08	273.01	45.96	18.548
244.11	283.85	49.50	22.026
254.19	291.77	53.96	26.858
264.22	300.84	59.21	32.877
274.29	309.43		

sample were again fitted to polynomials in temperature by a least-squares method. The derived thermodynamic functions are given in Tables 6–8. These values are considered to have a probable error of less than 0.1% above 100 K.

DISCUSSION

Figure 2 is a deviation plot comparing the heat capacity measurements on natural and synthetic samples of pyrope and grossular. In calculating the deviations between the natural and synthetic pyrope, the heat capacity of the natural sample was based on the formula weight of pure pyrope (403.127 g mol^{-1}). The natural grossular values were treated similarly by WESTRUM et al. (1979). Neither data set for the natural samples has been corrected for deviations from end-member composition. In both cases the values for the synthetic samples are significantly greater over most of the measured range than those of the uncorrected natural samples, although an adjustment to end-member composition would be expected to account for much of the discrepancies.

Pyrope

The heat capacity values measured on the natural pyrope garnet in the lowest temperature region require a comment. Figures 1 and 2 show that the heat capacity does not smoothly approach zero as T → 0 K. The 18.8 mol% almandine content of

the garnet may be partly responsible. Almandine is known to undergo paramagnetic to antiferromagnetic ordering at 7.5 K (Prandl, 1971) for which the theoretical entropy contibution is 3R ln(2S + 1) = 40.14 J mol^{-1}K^{-1} (KITTEL, 1976; ULBRICH and WALDBAUM, 1976). The apparent anomaly may represent the high-temperature tail of this transition. At higher temperatures, the adjustment to end-member composition will be dominated by the almandine contribution. Because the correction will be large and because various methods of estimating the almandine heat capacity vary widely in results, no attempt was made to correct the heat capacity of the natural pyrope sample for additional components. Much of the discrepancy may be removed, however, by such a correction. KOLESNIK et al. (1977) give a corrected value for $C_{p,298} = 320.24$ J mol^{-1} K^{-1} which is 1.5% low in comparison to our measurements on synthetic pyrope.

A value of $S^{\circ}_{298} = 268$ J mol^{-1} K^{-1} based on the univariant reaction enstatite + spinel = pyrope + forsterite was calculated by NEWTON et al. (1977b). The absence of a heat capacity anomaly and the relatively good agreement between the observed S°_{298} and the value calculated from phase equilibrum studies is strong evidence against Mg^{2+} positional disorder as proposed by ZEMANN and ZEMANN (1961) and KLEBER et al. (1969) from X-ray studies.

Grossular

In the natural grossular FeO and H$_2$O are the major additional oxides attributed by WESTRUM et al. (1979) to almandine and hydrogrossular components, respectively. The C$_p$ values, adjusted to end-member composition at temperatures > 100 K by WESTRUM et al. (1979), are shown by solid triangles in Fig. 2. Unfortunately, the corrections increase the deviation with regard to the synthetic sample, KRUPKA et al. (1979), in a differential scanning calorimetry study on synthetic grossular and a natural grossular of similar composition to that used by WESTRUM et al. (1979), also observed lower heat capacities for the natural sample in the temperature range 350–700 K. The synthetic grossular in their study was crystallized hydrothermally from a gel at 923 K and 517 bar, a synthesis procedure quite different from the one in the present work. They did not detect a significant difference in the heat capacities of their natural and synthetic samples in the higher temperature (700–1000 K) section of their study. At least part of the difference in behavior of the corrected natural grossular and the synthetic shown in Fig. 2. could relate to the heat capacity approximation for hydrogrossular used by WESTRUM et al. (1979). It is probable from structural considerations that the use of brucite to model hydroxyls in a hydrogarnet, as was done by these authors, over-estimates their contribution to the heat capacity (A. B. THOMPSON, personal communication, 1979). A differential scanning calorimetry study might readily resolve this point.

Table 6. Molar thermodynamic functions of pyrope, $Mg_3Al_2Si_3O_{12}$, formula weight = 403.127 g mol^{-1}

T	C_p	$(S^\circ_T - S^\circ_0)$	$(H^\circ_T - H^\circ_0)$	$-(G^\circ_T - H^\circ_0)/T$
K	J $mol^{-1}K^{-1}$	J $mol^{-1}K^{-1}$	J mol^{-1}	J $mol^{-1}K^{-1}$
5	0.004	0.000	0.008	0.000
10	0.038	0.013	0.084	0.004
15	0.238	0.054	0.657	0.013
20	0.862	0.197	3.171	0.038
25	2.146	0.510	10.376	0.096
30	4.251	1.075	26.016	0.209
35	7.222	1.946	54.333	0.389
40	11.054	3.151	99.667	0.657
45	15.707	4.711	166.239	1.017
50	21.108	6.640	257.99	1.481
60	33.631	11.565	530.11	2.732
70	47.610	17.786	935.42	4.442
80	62.668	25.117	1485.91	6.540
90	78.41	33.405	2191.2	9.058
100	94.27	42.484	3054.3	11.941
110	110.17	52.216	4076.5	15.154
120	125.98	62.480	5257.6	18.669
130	141.59	73.18	6595.7	22.447
140	156.82	84.22	8088.1	26.464
150	171.54	95.56	9730.7	30.690
160	185.69	107.07	11517.3	35.104
170	199.16	118.74	13441.9	39.681
180	212.00	130.50	15498.0	44.401
190	224.22	142.30	17679.9	49.241
200	235.85	154.10	19980.3	54.191
210	246.90	165.85	22393	59.229
220	257.48	177.61	24916	64.35
230	267.57	189.28	27543	69.54
240	277.23	200.87	30267	74.77
250	286.48	212.38	33087	80.04
260	295.31	223.76	35995	85.35
270	303.72	235.10	38991	90.67
280	311.71	264.27	42070	96.02
290	319.32	257.36	45225	101.42
300	326.60	268.28	48455	106.78
310	333.59	279.11	51756	112.17
320	340.37	289.83	55124	117.57
330	347.02	300.41	58563	122.93
340	353.63	310.87	62065	128.32
350	360.20	321.21	65634	133.68
273.15	306.27	238.61	39953	92.34
298.15	325.31	266.27	47852	105.77

Table 7. Molar thermodynamic functions of grossular, $Ca_3Al_2Si_3O_{12}$, formula weight = 450.452 g mol^{-1}

| T	C_p	$(S_T^\circ - S_0^\circ)$	$(H_T^\circ - H_0^\circ)$	$-(G_T^\circ - H_0^\circ)/T$
K	J mol^{-1}K^{-1}	J mol^{-1}K^{-1}	J mol^{-1}	J mol^{-1}K^{-1}
5	0.013	0.004	0.017	0.000
10	0.071	0.029	0.218	0.008
15	0.293	0.092	1.021	0.025
20	0.803	0.238	3.619	0.059
25	1.715	0.506	9.719	0.117
30	3.167	0.937	21.661	0.213
35	5.322	1.577	42.568	0.360
40	8.293	2.473	76.258	0.565
45	12.100	3.661	126.897	0.841
50	16.707	5.167	198.602	1.197
60	27.886	9.167	419.61	2.171
70	41.058	14.431	762.91	3.535
80	55.789	20.861	1245.95	5.289
90	71.630	28.338	1882.42	7.422
100	87.738	36.719	2679.0	9.929
110	104.27	45.852	3638.8	12.774
120	120.88	55.639	4764.7	15.933
130	137.32	65.98	6055.9	19.380
140	153.43	76.74	7509.9	23.091
150	168.99	87.86	9122.4	27.037
160	183.97	99.24	10887.6	31.192
170	198.24	110.83	12799.3	35.535
180	211.84	122.55	14850.3	40.041
190	224.76	134.35	17033.5	44.693
200	237.07	146.19	19343.5	49.472
210	248.82	158.03	21774	54.363
220	260.04	169.87	24317	59.342
230	270.83	181.67	26974	64.392
240	281.17	193.43	29732	69.538
250	291.08	205.10	32593	74.726
260	300.58	216.69	35551	79.96
270	309.70	228.24	38606	85.23
280	318.40	239.66	41744	90.54
290	326.73	250.96	44970	95.90
300	334.64	262.17	48279	101.25
310	342.17	273.26	51664	106.61
320	349.41	284.26	55120	112.01
330	356.39	295.10	58651	117.36
340	363.34	305.85	62250	112.76
350	370.33	316.48	65915	128.16
273.15	312.50	231.84	39585	86.90
298.15	333.17	260.12	47660	100.25
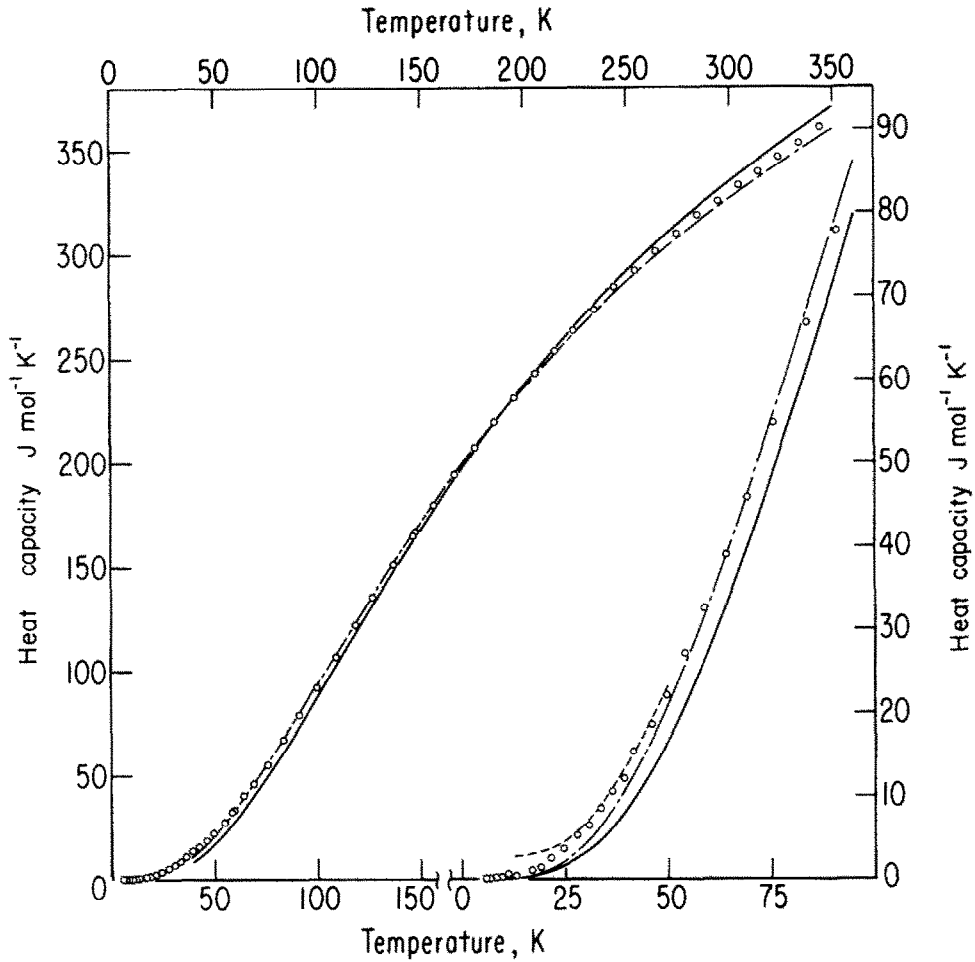
Fig. 1. Molar heat capacities of synthetic pyrope, grossular, and pyrope$_{60}$grossular$_{40}$. Circles are the data points for the mix crystal. Smoothed values are given for grossular——— and pyrope———, Smoothed values for natural pyrope, adjusted to the formula weight of pyrope, are given by a dashed line at T < 50 K. The lower temperature region has been expanded at the right.
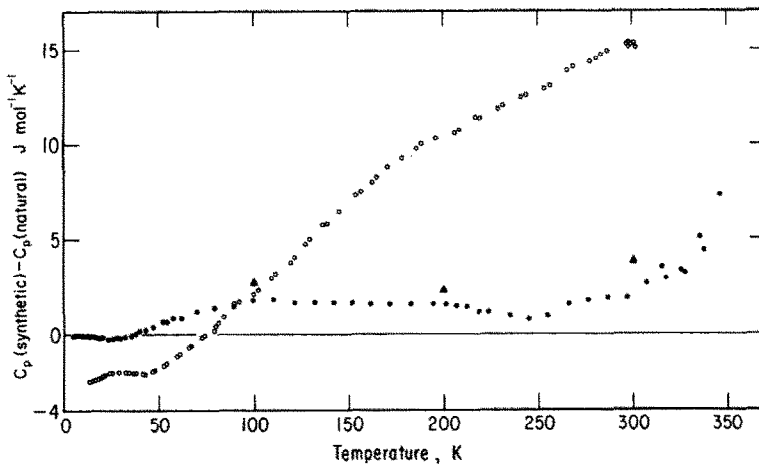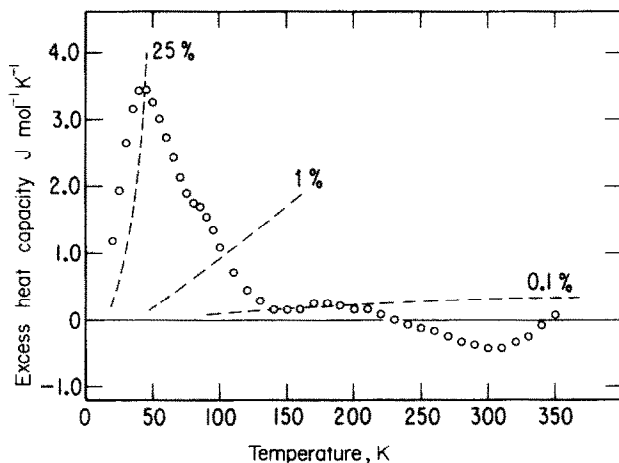

Fig. 2. Deviation plot. Differences between natural and synthetic samples of pyrope and grossular are given by

$$\Delta C_p = C_p(\text{synthetic}) - C_p(\text{natural}).$$

Open circles are for pyrope; solid circles are for grossular. Natural grossular values, adjusted to end-member composition, are indicated at three temperatures by solid triangles.

Table 8. Molar thermodynamic functions of pyrope$_{60}$grossular$_{40}$, $Mg_{1.8}Ca_{1.2}Al_2Si_3O_{12}$, formula weight $= 422.057$ g mol^{-1}

T	C_p	$(S_T^o-S_0^o)$	$(H_T^o-H_0^o)$	$-(G_T^o-H_0^o)/T$
K	J mol^{-1}K^{-1}	J mol^{-1}K^{-1}	J mol^{-1}	J mol^{-1}K^{-1}
5	.000	.008	.033	.000
10	.188	.050	.385	.013
15	.799	.222	2.628	.050
20	2.017	.602	9.389	.134
25	3.912	1.247	23.932	.289
30	6.460	2.176	49.597	.523
35	9.615	3.397	89.538	.841
40	13.355	4.920	146.725	1.251
45	17.686	6.740	224.10	1.757
50	22.610	8.853	324.60	2.360
60	34.054	13.958	606.35	3.849
70	47.120	20.171	1011.02	5.728
80	61.668	27.393	1553.65	7.975
90	77.24	35.560	2248.5	10.577
100	92.759	44.497	3098.3	13.514
110	108.53	54.078	4104.5	16.765
120	124.39	64.18	5268.9	20.292
130	140.16	74.77	6591.9	24.075
140	155.65	85.73	8071.4	28.083
150	170.71	96.99	9703.5	32.300
160	185.18	108.49	11483.4	36.702
170	199.03	120.12	13405.1	41.267
180	212.17	131.88	15461.6	45.974
190	224.64	143.68	17646.0	50.802
200	236.52	155.52	19952.2	55.743
210	247.82	167.32	22376	60.777
220	258.57	179.08	24907	65.90
230	268.86	190.83	27543	71.04
240	278.74	202.46	30284	76.27
250	288.19	214.05	33116	81.59
260	297.23	225.52	36045	86.90
270	305.85	236.90	39062	92.22
280	314.05	248.15	42162	97.61
290	321.92	259.32	45342	102.97
300	329.41	270.37	48597	108.37
310	336.60	281.29	51928	113.76
320	343.63	292.09	55329	119.20
330	350.54	302.75	58798	124.60
340	357.44	313.34	62342	130.00
350	364.34	323.80	65948	135.35
273.15	308.49	240.45	40028	93.93
298.15	328.03	268.32	47990	107.36

Fig. 3. Excess heat capacity of pyrope$_{60}$grossular$_{40}$ compared to a linear combination of the end member heat capacities. Percentages are based on the linear combination.

C_p(excess) $= C_p$(pyrope$_{60}$grossular$_{40}$) $- [0.6C_p$(pyrope) $+ 0.4C_p$(grossular)].

$Pyrope_{60}grossular_{40}$

The excess heat capacity of the $pyrope_{60}grossular_{40}$ composition shown in Fig. 3 is based on a linear combination of the end-member heat capacities. Though the greatest excess heat capacity, 25% of the linear combination, occurs at 40–45 K, the relative contribution is greater at lower temperatures. Above 115–120 K the excess heat capacity is within the experimental error. The accumulated $S^{es}_{298.15} - S_0$ is 4.5(3) J mol^{-1} K^{-1}. This value can be compared to an excess of 13.0 J mol^{-1} K^{-1} estimated by HENSEN *et al.* (1975) from phase equilibrium experiments which were limited to pyrope-rich compositions. By analogy with the excess entropy of mixing calculated by THOMPSON and HOVIS (1979) in the analbite–sanidine series, the maximum excess may be displaced to grossular-rich compositions. Without additional information, however, any asymmetry cannot be assessed.

The excess heat capacity of the $pyrope_{60}grossular_{40}$ composition and the apparently high heat capacity of pyrope may be related to the coordination of magnesium in garnets. GIBBS and SMITH (1965) reported a larger than expected thermal ellipsoid for Mg^{2+} which was attributed to its unusually large, eight-fold coordination. In the solid solution, the occupation of this structural position in part by calcium might expand it, increasing the vibrational amplitude of the magnesium ions and their contribution to the heat capacity. This trend can be observed in the low-temperature in Fig. 1.

Note added in proof

Very recently KOLESNIK *et al.* (*Geokhimiya*, 1979, 713–721) have published heat capacity data (13–300 K) for a natural grossular sample. At 298 K, $C_p = 334.26$ J mol^{-1} K^{-1} and $S^\circ = 259.78$ J mol^{-1} K^{-1}. The composition of the sample is very close to end-member grossular, and the thermophysical functions at 298 K agree within error with those of the synthetic grossular in the present study.

REFERENCES

BURNHAM C. W. (1962) Lattice constant refinement. *Carnegie Inst. Washington Yearb.* **61**, 132–135.

Commission on atomic weights, I.U.P.A.C. (1976) Atomic weights of the elements 1975. *Pure Appl. Chem.* **47**, 75–95.

GIBBS G. V. and SMITH J. W. (1965) Refinement of the crystal structure of synthetic pyrope. *Am. Mineral.* **50**, 2023–2039.

HENSEN B. J., SCHIMD R. and WOOD B. J. (1975) Activity–composition relations for pyrope–grossular garnet. *Contrib. Mineral. Petrol.* **51**, 161–166.

KISELEVA I. A., TOPOR N. D. and MELCHAKOVA L. V. (1972) Experimental determination of heat content and heat capacity in grossular, andradite and pyrope. *Geokhimiya* 1372–1379.

KITTEL C. (1976) *Introduction to Solid State Physics*, 5th edn, 599 pp. Wiley.

KLEBER W., JOST K. H. and ZIEMER B. (1969) Zur Koordination des Magnesiums in Pyrop und Untersuchungen uber dessen thermische Zersetzung. *Krist. Tech.* **4**, 423–429.

KOLESNIK Y. N., NOGTEVA V. V. and PAUKOV I. E. (1977) Heat capacity of pyrope within the temperature ranges of 13–300°K. Thermodynamical properties of some natural garnets. *Geokhimiya* 533–541.

KRUPKA K. M., ROBIE R. A. and HEMINGWAY B. S. (1979) High-temperature heat capacities of corundum, periclase, anorthite, $CaAl_2Si_2O_8$ glass, muscovite, pyrophyllite, $KAlSi_3O_8$ glass, grossular, and $NaAlSi_3O_8$ glass. *Am. Mineral.* **64**, 86–101.

NEWTON R. C., CHARLU T. V. and KLEPPA O. J. (1977a) Thermochemistry of high pressure garnets and clinopyroxenes in the system $CaO–MgO–Al_2O_3–SiO_2$. *Geochim. Cosmochem. Acta* **41**, 369–377.

NEWTON R. C., THOMPSON A. B. and KRUPKA K. M. (1977b) Heat capacity of synthetic $Mg_3Al_2Si_3O_{12}$ from 350–1000 K and the entropy of pyrope. EOS, *Trans. Am. Geophys. Union* **58**, 523.

PRANDL W. (1971) Die magnetische struktur und die atomparameter des almandins $Al_2Fe_3(SiO_4)_3$. *Z. Kristallogr.* **134**, 333–343.

THOMPSON J. B. and HOVIS G. L. (1979) Entropy of mixing in sandine. *Am. Mineral.* **64**, 57–65.

TOPOR N. D., KIESELEVA I. A. and MELCHAKOVA L. V. (1972) Measurement of the heat content of minerals by the method of high temperature microcalorimetry. *Geokhimiya* 335–343.

ULBRICH H. H. and WALDBAUM D. R. (1976) Structural and other contributions to the third-law entropies of silicates. *Geochim. Cosmochim. Acta* **40**, 1–24.

WESTRUM E. F. JR, FURUKAWA G. T. and McCULLOUGH J. T. (1968) Adiabatic low-temperature calorimetry. In *Experimental Thermodynamics* (eds. J. T. McCullough and D. W. Scott), pp. 133–214. Butterworths.

WESTRUM E. F. JR, ESSENE E. J. and PERKINS D. III (1979) Thermophysical properties of the garnet, grossularite, $(Ca_3Al_2Si_3O_{12})$. *J. Chem. Thermodyn.* **11**, 57–66.

ZEMANN A. and ZEMANN A. (1961) Vereinerung der Kristallstruktur von synthetischen Pyrop, $Mg_3Al_2(SiO_4)_3$. *Acta Crystallogr.* **14**, 835–837.